Ectopic Expression of Hel-N1, an RNA-Binding Protein, Increases Glucose Transporter (GLUT1) Expression in 3T3-L1 Adipocytes

RENU G. JAIN,[1] LUCY G. ANDREWS,[2] KEVIN M. McGOWAN,[1] PHILLIP H. PEKALA,[1]*
AND JACK D. KEENE[2]

*Department of Biochemistry, School of Medicine, East Carolina University, Greenville, North Carolina 27834,[1] and
Department of Microbiology, Duke University Medical Center, Durham, North Carolina 27710[2]*

3T3-L1 preadipocytes ectopically expressing the mammalian RNA-binding protein Hel-N1 expressed up to 10-fold more glucose transporter (GLUT1) protein and exhibited elevated rates of basal glucose uptake. Hel-N1 is a member of the ELAV-like family of proteins associated with the induction and maintenance of differentiation in various species. ELAV proteins are known to bind in vitro to short stretches of uridylates in the 3′ untranslated regions (3′UTRs) of unstable mRNAs encoding growth-regulatory proteins involved in transcription and signal transduction. GLUT1 mRNA also contains a large 3′UTR with a U-rich region that binds specifically to Hel-N1 in vitro. Analysis of the altered GLUT1 expression at the translational and posttranscriptional levels suggested a mechanism involving both mRNA stabilization and accelerated formation of translation initiation complexes. These findings are consistent with the hypothesis that the Hel-N1 family of proteins modulate gene expression at the level of mRNA in the cytoplasm.

Interaction of RNA-binding proteins with *cis* elements in mRNAs is believed to be involved in regulation of their stability and translational efficiency (reviewed in reference 32). The regulated stability of transferrin, granulocyte-macrophage colony-stimulating factor, and histone mRNAs has been shown, at least in part, to be controlled by the binding of specific proteins to consensus sequences in the 3′ untranslated region (3′UTR) of these messages (3, 37, 41). Studies of tobacco mosaic virus, the *Drosophila melanogaster* developmental gene *hunchback*, human cytokine, and 15-lipoxygenase mRNAs have demonstrated that the 3′UTR also contains information capable of regulating translational efficiency which may be mediated by RNA-binding proteins (13, 25, 35, 36). A major class of RNA-binding proteins which possess an 80-amino-acid consensus element, termed the RNA recognition motif (RRM) (39), which forms the core of a functional RNA-binding domain has been identified.

Hel-N1 (human embryonic lethal abnormal vision [ELAV]-like neuronal protein 1), a mammalian homolog of *Drosophila* ELAV, is an mRNA-binding protein of the RRM family (15, 16, 27). Recent studies on Hel-N1, and the alternative form, Hel-N2 (lacking a 13-amino-acid segment between RRM2 and RRM3), in human medulloblastoma cells and embryonic carcinoma P19 cells have indicated that it plays a role in mRNA metabolism (15). These proteins are bound to poly(A)$^+$ mRNA in granular RNP structures, and their expression is upregulated during neuronal cell differentiation of P19 cells (15). Likewise, hNT2 cells when induced to differentiate by retinoic acid exhibited a marked increase in the expression of human ELAV-like proteins which colocalized with mRNPs associated with polysomes (1). Hence, data from both of these studies support an important role for mammalian ELAV-like proteins in the processes of cell growth and differentiation.

Interestingly, members of the ELAV family have been shown to bind the AU-rich regions of the 3′UTRs in cytokine and proto-oncogene mRNAs (5, 14, 27). In vitro binding studies with Hel-N1 documented preferential binding to the 3′UTRs of mRNAs which have short stretches of uridylate residues; however, in vivo RNA targets of ELAV proteins have not been identified (27). A combinatorial library representing naturally derived 3′UTRs was used to define brain mRNA binding targets of Hel-N1 by in vitro iterative selection (14). This approach allowed the identification of potential mRNA binding targets which included transcripts encoding certain tumor markers, transcription factors and growth regulatory proteins.

Previous attempts to transfect various mammalian cell lines such as B104, NIH 3T3, and COS with Hel-N1 resulted in cessation of cellular proliferation and/or dramatic morphological changes, precluding analysis of specific effects of Hel-N1 expression. In this study, we have examined the effect of ectopic expression of Hel-N1 on the expression of specific genes in the 3T3-L1 cell system. As adipocytes, these cells express two glucose transporters: GLUT1, a basal, growth-related transporter; and GLUT4, the insulin-responsive glucose transporter. Characterization of adipocytes expressing Hel-N1 demonstrated an increased content of GLUT1 protein with no alteration in the expression of GLUT4. Control of the increase in GLUT1 content resides with translational (acceleration of the formation of the translation initiation complexes) and posttranscriptional (GLUT1 mRNA stability) mechanisms. Furthermore, Hel-N1 was demonstrated to bind in vitro to the AU-rich 3′UTR of GLUT1 mRNA. We propose that Hel-N1 may compete with endogenous factors that normally regulate mRNA translation or stability, giving rise to the secondary effects on gene expression.

MATERIALS AND METHODS

Materials. Dulbecco's modified Eagle's medium was purchased from Gibco Laboratories, Grand Island, N.Y. Bovine and fetal bovine sera were purchased from HyClone, Logan, Utah. All radiolabeled compounds were obtained from New England Nuclear, Boston, Mass., or ICN Biomedicals Inc., Irvine, Calif. GLUT1 and GLUT4 antibodies were prepared and characterized as previously described (22). The 3T3-L1 cells used in these experiments were obtained from

* Corresponding author. Phone: (919) 816-2684. Fax: (919) 816-3383. E-mail: pekala@brody.med.ecu.edu.

Howard Green, Harvard University, Boston, Mass. Hybond-N and Hybond-NT were obtained from Amersham, Arlington Heights, Ill. Protogel and Sequagel were obtained from National Diagnostics. All other chemicals unless otherwise specified were of molecular biology grade and purchased from Sigma, St. Louis, Mo.

3T3-L1 cell culture. Murine 3T3-L1 preadipocytes were cultured, maintained, and differentiated as previously described (42). Optimal differentiation was observed by using a protocol that involved exposure of 3T3-L1 cells (day 0 = 2 days postconfluence) and transfectants to fetal bovine serum (10%), insulin (1 μg/ml), 1 μM dexamethasone (DEX), and 0.5 mM 3-isobutyl-1-methylxanthine (MIX). Two days later, the culture medium was changed to medium lacking MIX and DEX for maintenance of the cells in insulin. After 2 days, the concentration of insulin was decreased to 250 ng/ml; 48 h later, insulin was omitted.

Determination of 2-deoxyglucose uptake. Assay of [³H]2-deoxyglucose uptake was performed as we have described previously (38, 45). Results of such an assay have been shown to approximate the actual hexose uptake rate in the 3T3-L1 adipocytes (11).

RNA isolation and analysis. Total RNA was isolated from the cells by extraction with guanidine isothiocyanate and centrifugation through 5.7 M cesium chloride as described by Chirgwin et al. (4). Northern analysis was performed as previously described (7, 42). Half-life determinations of the mRNA were performed as described by Tebbey et al. (45).

Cell fractionation and GLUT1 and GLUT4 immunoblot analysis. Plasma and intracellular membranes were separated and characterized as we have previously described (42). Routinely, the microsomal phosphatase described by Klip and Walker (24) was used as a marker for the intracellular membrane fraction. Relative to the initial cell homogenate, a 28-fold purification with a 6.5% yield of the phosphatase was obtained. As a marker for plasma membranes, γ-glutamyl-transferase was used (12). Recovery of this marker enzyme was approximately 10% with a purification of 60-fold. Immunoblot analysis was carried out as we have described previously (42).

DNA probes. The cDNAs used in these studies were as follows: GLUT1, a 2.7-kb *Eco*RI fragment encoding the murine 3T3-L1 homolog of the HepG2/brain glucose transporter (20); GLUT4, a 1.8-kb *Eco*RI fragment encoding the 3T3-L1 homolog of the adipose/muscle (insulin-responsive) glucose transporter (20); and β-actin, a 1.9-kb *Hin*dIII fragment obtained from D. W. Cleveland, The Johns Hopkins University School of Medicine, Baltimore, Md. (6).

Transfections. The cells were cotransfected at 50% confluence by the calcium phosphate precipitation method with plasmids pSV₂neo and pBC-Hel-N1 in a 1:10 ratio. Clones were selected on the basis of resistance to the aminoglycoside G418 (400 μg/ml; active), pooled, passaged twice, and used in the described experiments. Three individual transfections were performed, with a mean of 11 ± 3 clones pooled, the three derived cell lines exhibited the same phenotype, and all experiments were performed with expansions of these original clones.

Construction of plasmids. The Hel-N1-expressing plasmid used for transfection of 3T3-L1 preadipocytes was derived from the pBC/CMV/IL2 vector (10). The human interleukin-2 cDNA sequence of this vector was replaced with the cDNA encoding a fusion protein consisting of a 12-amino-acid T7 phage gene 10 (g10) epitope tag (44) in frame with U1-70K cDNA (40). The U1-70K sequence was removed by restriction digestion and replaced by a 1,656-nucleotide (nt) Hel-N1 sequence consisting of the protein coding region and the 3′UTR. The Hel-N1 sequence, inserted at the *Bam*HI site downstream of the g10 tag, was excised from the vector used for expression of Hel-N1 protein in *Escherichia coli* (23).

Preparation and isolation of regions of the GLUT1 3′UTR based on A+U content. The GLUT1 3′UTR was divided into five regions based on A+U content. Each region was amplified by PCR techniques. The 5′ primer contained the sequence of the T7 promoter for the preparation of riboprobes for RNA gel shift assays and immunoprecipitation experiments. The GLUT4 3′UTR construct is bp 1590 to 2500 of the insulin-responsive glucose transporter contained within pBluescript (20). The plasmid was digested with restriction enzymes to produce templates for T3 transcripts containing the complete 3′UTR plus some coding region (*Xho*I) and progressively shorter sequences which remove potential binding sites for Hel-N1. Digestion with *Hin*dIII eliminates a 24-nt U-rich sequence (71% U, 81% A+U) containing a maximum of five contiguous uridylates. Digestion with *Tfi*I eliminates (in addition to the above U-rich sequence) the only AUUUA pentamer which occurs in the 3′UTR of GLUT4.

In vitro analysis of RNA-protein interactions. RNA transcripts labeled with [α-³²P]UTP were prepared as previously described (27). Immunoprecipitation of Hel-N1-bound RNAs, using partially purified T7 g10 epitope-tagged protein (46) and either anti-g10 or anti-Hel-N1 rabbit polyclonal antibodies (14), was performed as described previously (27) except that the amount of protein A beads per reaction was reduced to 1 mg. Electrophoretic gel mobility assays were performed as previously described (27) except that [α-³²P]UTP-labeled GLUT1 and GLUT4 sequences were resolved by high-ionic-strength polyacrylamide gel electrophoresis (PAGE) (2).

Analysis of Hel-N1 expression in transfected 3T3-L1 cells. RNA, DNA, and protein were isolated from cultured 3T3-L1 cells by using TriReagent (Molecular Research Center, Inc.) as instructed by the manufacturer.

(i) DNA. Two hundred nanograms of cellular DNA was used as the template for PCR performed with primers complementary to sequences in the 5′ and 3′ termini of the protein coding region of the Hel-N1 insert in the pBC expression

vector (sequences below). PCR products were resolved on a 1% agarose gel and detected with ethidium bromide.

(ii) RNA. Five micrograms of total cellular RNA was used for reverse transcription (RT) followed by PCR (RT-PCR) as described previously (18), using random hexamers to prime the RT reaction. The RT products were then used for two rounds of PCR amplification using nested oligonucleotide primers spanning the region between the N-terminal T7 phage g10 epitope tag and the end of the coding region. The outer set of primers consisted of the following: forward primer (G10, complementary to the T7 phage g10 epitope tag), 5′ CATATGG CTAGCATGACT 3′; and reverse primer (HE/AS11, complementary to the end of coding of Hel-N1), 5′ GGGGGAATTCCTAGGCTTTGTGCGTTTTG 3′. The inner set of nested primers consisted of the following: forward primer (HE/AS12, complementary to the start of coding of Hel-N1), 5′ GCGCCGCC ATGGAAACACAAGTGTC 3′; and reverse primer (HE/AS29, complementary to the end of the coding region of Hel-N1 overlapping HE/AS11), 5′ TAGTC GAATTCGGCTTTGTGCGTTTTGTT 3′. Reaction conditions were identical for both set of primers: 30 cycles of 94°C for 1 min, 50°C for 1 min, and 72°C for 2 min. One-fourth (5 μl) of the RT reaction product was used as the template for the first round of PCR. Three microliters of the product of the second round of PCR was resolved on a 1% agarose gel and detected by ethidium bromide. All RNAs were transcribed in the presence and absence of reverse transcriptase to detect any possible contamination by DNA.

(iii) Protein. Proteins were separated by sodium dodecyl sulfate (SDS)-PAGE (10% gel) and electrotransferred to a Hybond-ECL nitrocellulose membrane (Amersham). The membranes were processed as instructed by the manufacturer, and the proteins were detected by enhanced chemiluminescence. When comparisons between control and transfected cell lines were made, the analysis was performed on separate gels on the same apparatus at the same time. The individual blots generated were probed simultaneously.

Polysome profiles: analysis of polysomes by sucrose density gradients. Polysome profiles were generated as described by Long and Pekala (28). Briefly, three 10-cm-diameter plates of 3T3-L1 adipocytes were used for each polysome distribution analysis. Cells were washed twice with ice-cold phosphate-buffered saline containing 100 μg of cycloheximide per ml and lysed by the addition of 200 μl of polysome lysis buffer (100 mM KCl, 5 mM MgCl₂, 10 mM HEPES [pH 7.4], 100 μg of cycloheximide per ml, 0.5% Nonidet P-40). The lysate was transferred to a 1.5-ml microcentrifuge tube and passaged three to four times through a 27-gauge needle to ensure cell lysis. Nuclei were pelleted by centrifugation at 4°C and 12,000 × g for 5 min. The supernatant was then subjected to centrifugation one more time to ensure the removal of any nuclei. The resulting supernatant was layered on a linear 15 to 45% (wt/vol) sucrose gradient in polysome gradient buffer (100 mM KCl, 5 mM MgCl₂, 10 mM HEPES [pH 7.4]), and gradients were centrifuged at 35,000 rpm for 2 h at 4°C in a Beckman SW41 rotor. Gradient fractions were collected with a Brandel model 184 density gradient fractionator. RNA was purified from the sucrose gradient fractions by proteinase K digestion followed by phenol extraction. Each sample was diluted with an equal volume of a proteinase K solution (0.2 M Tris-Cl [pH 7.5], 25 mM EDTA, 0.3 M NaCl, 2% SDS, and 250 μg of proteinase K per ml). Samples were incubated at 45°C for 30 min and then extracted first with phenol-chloroform and then with chloroform alone. The aqueous phase was recovered, and the RNA was precipitated with 0.3 M sodium acetate (pH 5.2) and 2.5 volumes of ethanol. GLUT1 mRNA was analyzed by RNase protection assay.

RNase protection assay. The RNase protection assay was performed by using an RPA II assay kit (Ambion, Austin, Tex.) as instructed by the manufacturer. The GLUT1 RNase protection assay probe contains the *Hin*cII-*Hin*dIII fragment of the GLUT1 coding region. The total probe size is approximately 290 bases. The protected fragment is 257 bp.

Triglyceride assay. The triglyceride assay was performed with a triglyceride kit (Sigma Diagnostics, St. Louis, Mo.). Consistent with other experiments performed in these studies, two 10-cm-diameter plates were harvested on day 8 of the differentiation program.

Nucleotide sequence accession numbers. The cDNA sequences of GLUT1 and GLUT4 are deposited in GenBank under accession numbers M23384 and M23383, respectively.

RESULTS

Characterization of stable 3T3-L1 transfectants expressing Hel-N1. Stable transfectants expressing Hel-N1 were prepared by the calcium phosphate precipitation method. After selection, based on G418 resistance, clones were combined, passaged twice, and replated, and differentiation relative to that of untransfected 3T3-L1 cells was monitored (Fig. 1). Quantification of triacylglycerol content on day 8 after induction of differentiation demonstrated that the Hel-N1 transfectants accumulated 40% more lipid than controls: 0.160 ± 0.002 (mean ± standard deviation [SD]) and 0.220 ± 0.005 μmol of triacylglycerol/10⁶ cells for untransfected and Hel-N1-transfected cells, respectively. This difference is significant by Stu-
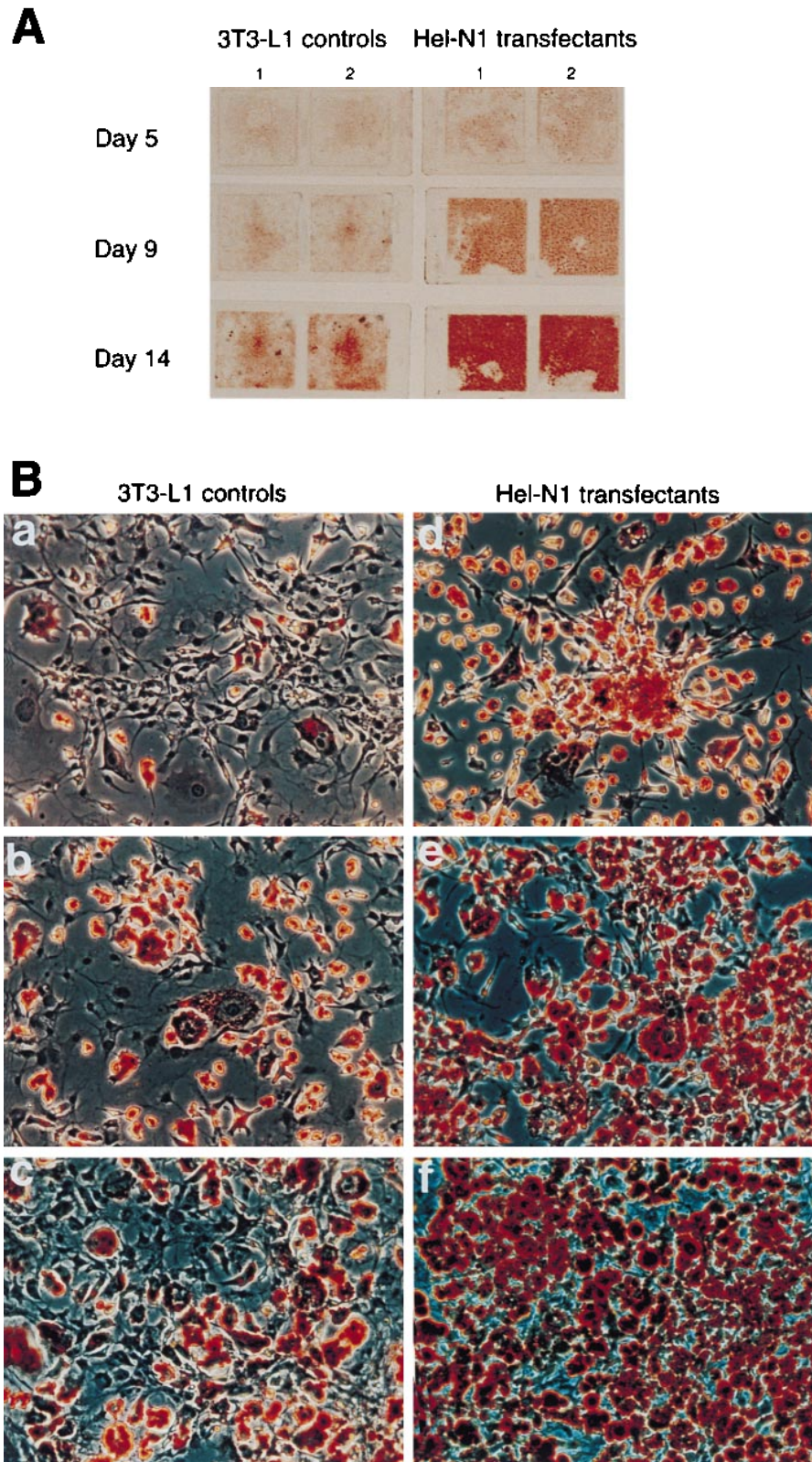
FIG. 1. Effect of expression of rHel-N1 on 3T3-L1 adipocyte conversion. (A) Macroscopic appearance of oil red O-stained two-well chamber slides on which cells were induced to differentiate. Inductions were performed in duplicate (wells 1 and 2) for each time point for both cell lines, and the slides were fixed on days 5, 9, and 14 following exposure to inducing agents. No difference between untransfected and Hel-N1-transfected cells was discernible on day 1. (B) Microscopic appearance of cells on the slides in panel A. Representative areas at low power of untransfected cells (a to c) and Hel-N1 transfectants (d to f) are shown on days 5 (a and d) 9 (b, and e), and 14 (c and f) following induction.
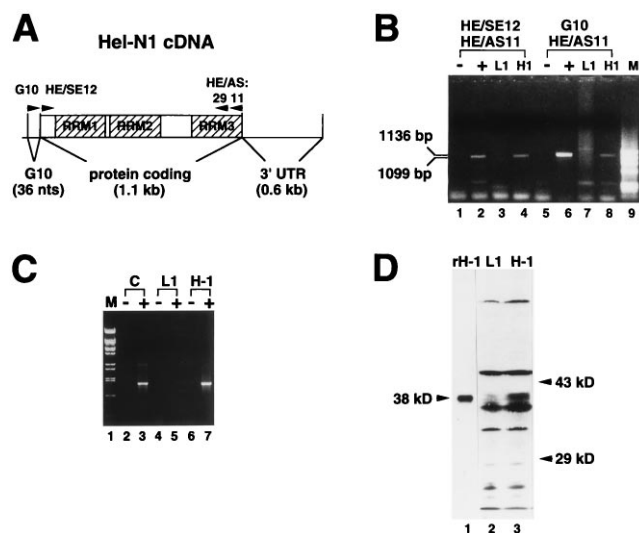
FIG. 2. Expression of Hel-N1 in transfected preadipocytes. (A) Schematic diagram of Hel-N1 protein and the cDNA inserted into the pBC expression vector. The locations of the primers used for PCR amplification are indicated (see Materials and Methods for primer sequences). (B) PCR analysis of genomic DNA isolated from untransfected and Hel-N1-transfected 3T3-L1 cells, using the two sets of primers diagrammed in panel A. Templates: lanes 1 to 4, HE/SE12 and HE/AS11; lanes 5 to 8, G10 (complementary to 18 nt of an N-terminal epitope tag expressed by the construct used to transfect 3T3-L1 cells) and HE/AS11. Lane 9, φX174/HaeIII marker. (C) RT-PCR analysis of total cellular RNA isolated from untransfected cells and Hel-N1 transfectants. Templates: Lane 2, none, lane 3, Hel-N1 plasmid (1 pg); lanes 4 to 7, RNA (5 µg), reverse transcribed and amplified by two rounds of nested PCR; lanes 4 and 6, untransfected samples prepared by using no reverse transcriptase; lanes 5 and 7, reverse transcriptase present. (D) Immunoblot of Hel-N1 protein in extracts prepared from untransfected 3T3-L1 cells and 3T3-L1 cells transfected with Hel-N1. Protein the size of Hel-N1 was detected in cells transfected with the Hel-N1 construct, using rabbit polyclonal antiserum to recombinant Hel-N1. A minor amount of cross-reactive protein of approximately the same size was detected in untransfected cells. Lanes: 1, rHel-N1 protein marker (5 ng); lane 2, protein (200 µg) isolated from untransfected 3T3-L1 cells at confluence; lane 3, protein (200 µg) isolated from Hel-N1 transfected cells at confluence.

dent's t test ($P < 0.05$). Morphologically, there appeared to be a more rapid onset of the adipocyte phenotype, which will be examined in greater detail in future studies. As shown in Fig. 1, a uniform distribution of the cells exhibiting the adipocyte phenotype among the pooled clones was observed. In contrast, 3T3-L1 cells transfected with other expression constructs followed by selection using G418 gave rise to a clonal rather than uniform differentiation (19).

Verification of the presence of the Hel-N1 DNA, RNA, and protein in the stable transfectants. The presence of the recombinant Hel-N1 (rHel-N1) DNA and RNA in the Hel-N1 transfectants and its absence from untransfected 3T3-L1 genomic DNA was confirmed by PCR and RT-PCR amplification, respectively. As shown in Fig. 2, specific primers were used to amplify the protein coding region of rHel-N1 cDNA. The data demonstrate the presence of rHel-N1 sequences in DNA isolated from Hel-N1-transfected 3T3-L1 cells (Fig. 2B, lanes 4 and 8) and its absence in the untransfected 3T3-L1 cells (lanes 3 and 7). In addition, the presence of the Hel-N1 mRNA was detected by RT-PCR as described in Materials and Methods (Fig. 2C). Primers complementary to a sequence within the N-terminal g10 epitope tag of the recombinant plasmid excluded the possibility of amplification of an endogenous murine homolog of Hel-N1.
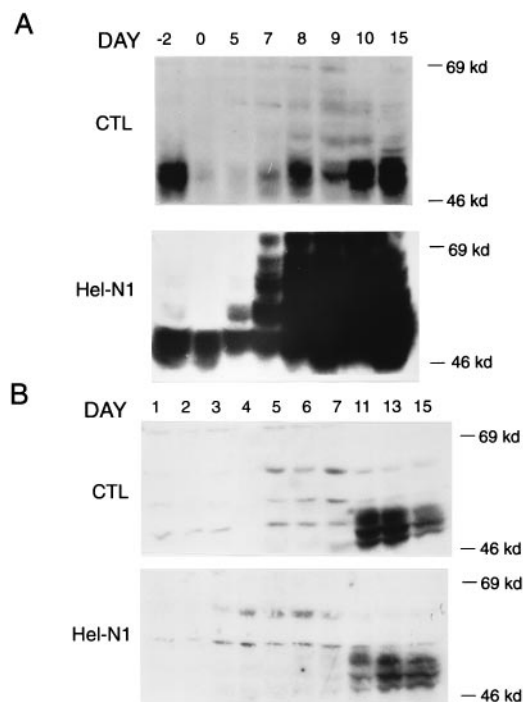

FIG. 3. Expression of glucose transporters GLUT1 and GLUT4. Shown are Western blots of cell extracts prepared from both untransfected 3T3-L1 cells and the Hel-N1 transfectants throughout the differentiation time course. Total cell extracts were prepared at each time point, and protein equivalent to 10^6 cells was analyzed by SDS-PAGE and immunoblotting. Blots were generated and probed with antibodies specific to GLUT1 (A) and GLUT4 (B). The data shown are representative of an experiment performed twice with each of two independent sets of transfected cells. Protein bands were quantified with Imagequant software (Molecular Dynamics, Sunnyvale, Calif.). CTL, control.

The presence of the Hel-N1 protein was detected by immunoblotting of cell extracts prepared from transfected and untransfected cells with rabbit polyclonal antiserum to rHel-N1 (14). As shown in Fig. 2D (lane 3), a protein of approximately 38 kDa, consistent with the size of epitope-tagged Hel-N1, was detected in the transfected cells at confluence, and no change in the level of expressed Hel-N1 protein was observed in fully differentiated adipocytes. Small amounts of cross-reactive proteins were also detected in the transfected and untransfected adipocytes (lanes 2 and 3).

Following verification of the presence of the Hel-N1 DNA, RNA, and expressed protein in the stable transfectants, studies were undertaken to determine the effect of Hel-N1 transfection on the expression of the glucose transporters which are characteristic of adipocyte cells.

Expression of GLUT1 and GLUT4 in the stable transfectants. Cell extracts were prepared as detailed in Materials and Methods, and protein from 10^6 cells was separated by SDS-PAGE and analyzed by immunoblotting. Extracts from cells were collected over a period from confluence (day -2) to fully differentiated (day 10 to 15). As a point of reference, these preadipocytes are considered 2 days postconfluent on day 0, when their differentiation program is accelerated by exposure to MIX, DEX, and insulin (see Materials and Methods). Blots were analyzed by using specific polyclonal antisera against GLUT1 and GLUT4 (Fig. 3). As shown in Fig. 3A, we observed in the Hel-N1 transfectants a major (8- to 10-fold) increase in the expression of the GLUT1 protein which correlated with the onset of the adipocyte phenotype. This increase
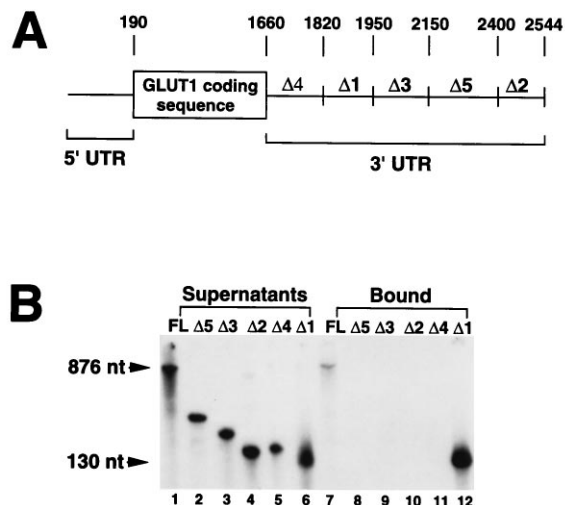
FIG. 4. Binding of Hel-N1 in vitro to sequences in the 3′UTR of GLUT1 mRNA. (A) Diagram of GLUT1 mRNA showing regions tested for binding to rHel-N1 protein. (B) Immunoprecipitation of rHel-N1 bound to radiolabeled transcripts of full-length GLUT1 3′UTR and segments within the 3′UTR, each represented by Δ. Lanes 1 to 6, ^{32}P-labeled transcripts remaining in the supernatants after the first step of binding; lanes 7 to 12, RNA bound to Hel-N1 after five washes.
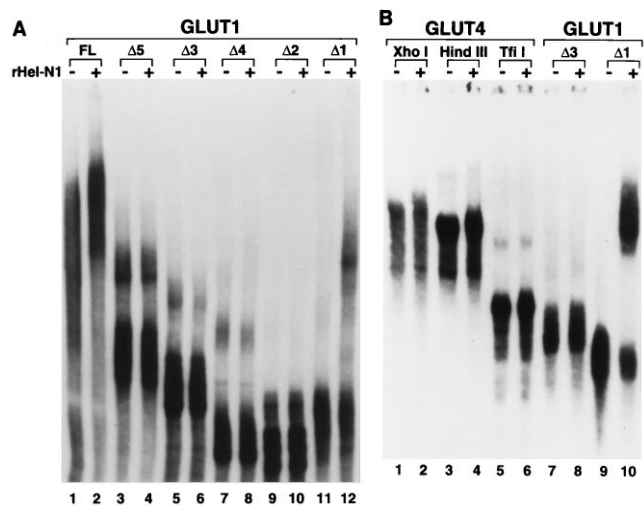

FIG. 5. Mobility shift assay of rHel-N1 binding in vitro to GLUT1 and GLUT4 transcripts. (A) RNA gel mobility assay of the GLUT1 transcripts diagrammed in Fig. 4A. Lanes 1, 3, 5, 7, 9, and 11, RNA only; lanes 2, 4, 6, 8, 10, and 12, RNA plus 0.5 µg of rHel-N1. (B) Gel retardation experiments using Hel-N1 and ^{32}P-labeled transcripts of GLUT4 3′UTR truncated at the indicated restriction enzyme sites is compared to binding (Δ1) and nonbinding (Δ3) sequences from the 3′UTR of GLUT1. Lanes 1, 3, 5, 7, and 9, RNA only; lanes 2, 4, 6, 8, and 10, RNA plus 0.5 µg of rHel-N1. The GLUT4 transcripts are 999 nt (full-length 3′UTR plus 3′ end of coding and polylinker cut at XhoI), 800 nt (HindIII truncation), and 316 nt (TfiI).

in GLUT1 expression did not occur in the absence of the hormone induction. To verify that the detected antigen was indeed all GLUT1, the same blot was stripped and reprobed with antiserum from which the GLUT1 antibody had been preabsorbed by using an antigen affinity column. Use of this antibody preparation resulted in a loss of detection of the antigen, confirming that the accumulated protein was GLUT1 (data not shown). The bands of various sizes observed in the Western blot analysis were believed to represent variations in the glycosylation state of the GLUT1 protein (30). We also noted that the expression pattern of GLUT1 in the 3T3-L1 cells during days 0 through 5 reflects a normal decrease in GLUT1 content, consistent with the cells being at confluence for several days prior to induction of differentiation (47).

For comparison, expression of the differentiation-specific glucose transporter, GLUT4, was not affected by expression of Hel-N1 (Fig. 3B). In parallel experiments, stable transfectants obtained by using truncated fragments of Hel-N1 (Hel-N2 and RRM3 [27]) did not exhibit a large increase in GLUT1 protein accumulation over the differentiation time course (data not shown).

In vitro binding of Hel-N1 to sequences in the 3′UTR of GLUT1 mRNA. RNA gel shift assays and immunoprecipitation experiments were performed to determine whether rHel-N1 could bind to the 3′UTR of GLUT1 mRNA. Sequences within the 887-base 3′UTR were amplified as five contiguous fragments by PCR using forward primers containing the T7 RNA polymerase promoter (Fig. 4A). Radiolabeled transcripts were prepared from the full-length 3′UTR as well as the fragments of the 3′UTR, and gel shifts and immunoprecipitations were performed as described in Materials and Methods. The results (Fig. 4B, lane 12; Fig. 5A, lane 12) demonstrate the binding of rHel-N1 to the Δ1 region (nt 1820 to 1950), which, as shown in Table 1, consists of a 68.5% A+U region, with specific subregions reaching as high as 73% A+U. No binding to the other four fragments of the GLUT1 3′UTR, which range from 37.5 to 69% A+U, was observed. The overall A+U content of the GLUT1 3′UTR is 49.3%. The results of binding of rHel-N1 to the other GLUT1 transcripts and their characteristics are sum-

marized in Table 1. Hel-N1 bound to the full-length 3′UTR (Fig. 5A, lane 1), but less full-length RNA than Δ1 RNA was immunoprecipitated on a molar basis (Fig. 4B, lane 7). The mobility of the full-length transcript shifted in the presence of rHel-N1 (Fig. 5A, lane 2) but because of the large size of this transcript (887 nt), it is difficult to compare it quantitatively with that of the Δ1 fragment. Recent experiments have further defined the binding site to a U-rich loop between positions 1911 and 1950 of GenBank sequence M23384, within the Δ1 construct. Various attempts to directly immunoprecipitate endogenous or exogenous Hel-N1 family proteins from whole cell extracts and to identify in vivo bound RNAs have not succeeded presumably because the epitopes on the endogenous proteins are not accessible in whole cell extracts.

As shown above, 3T3-L1 adipocytes express the insulin-responsive glucose transporter GLUT4, but its expression is not altered in Hel-N1-transfected cells. Radiolabeled probes for immunoprecipitation and gel shift assays were prepared from truncated portions of the 3′UTR of GLUT4 by restriction enzyme digestion as described in Materials and Methods. The overall A+U content of the GLUT4 3′UTR is 46.5%, while the HindIII truncation contains 43.5% A+U and the TfiI truncated transcript contains 41% A+U. The region that is most AU rich (55.5%) lies between the HindIII site and the end of the full-length GLUT4 3′UTR transcript (Table 1). The results of determinations of binding to these regions (Fig. 5B, lanes 1 to 6, and data not shown) demonstrate that Hel-N1 is not a ligand for the GLUT4 3′UTR, consistent with its showing no effect on GLUT4 expression in the differentiating Hel-N1 transfectants (Fig. 3B).

Analysis of GLUT1 mRNA levels during a differentiation time course. RNA from the untransfected cells and the stable transfectants was isolated at several time points in their differentiation time course as described in Materials and Methods. Upon Northern blot analysis of the RNA from the time course,

TABLE 1. Comparison of sequences Δ1 to Δ5 within the 3′UTR of GLUT1 mRNA and the region of greatest A/U richness within the 3′UTR of GLUT4

RNA transcripts[a]	Hel-N1 Binding	Longest A + U	Longest U-stretch	Percent A + U	#AUUUA Motifs
GLUT1 :					
Δ 1 Sequence (nts 1820-1950): UUCAGGACUUUGAUGGCUCCAGAAUUUUUAAUGAAAGCAAGACUGCUGCUCA GAUCUAUUCAGAUAAGCAGCAGGUUUUAUAAUUUUUUUUAUUACUGAUUUUGU UAUUUUUUUUUUUUAUCAGCCACUCUC	+	19	12	68.5[b]	0
Δ 2 Sequence (nts 2400-2544): GUGUAUAGAUGGAAGAUAUUUAUAUACUGGUUGUCAAUAUUAAAUACAGACA CUAAGUUAUAGUAUAUCUGGACAAACCCACUUGUAAAUACACCAACAAACUC CUGUAACUUUACCUAAGCAGAUAUAAAUGGCUGGUUUUUAG	−	11	5	69	1
Δ 3 Sequence (nts 1950-2150): CCUAUCUCCACACUGUAGUCUUCACCUUGAUUGGCCCAGUGCCUGAGGGUGG GGACCACGCCCUGUCCAGACACUUGCCUUCUUUGCCAAGCUAAUCUGUAGGG CUGGACCUAUGGCCAAGGACACACUAAUACCGAACUCUGAGCUAGGAGGCUU UACGCUGGAGGCGGUAGCUGCCACCCACUUCCGCAGGCCUGGACC	−	5	3	42.5	0
Δ 4 Sequence (nts 1660-1820): CAAGUGUGAGGAGCCCCACACCCAGCCCGGCCUGCUCCCUGCAGCCCAAGGA UCUCUCUCGGAGCACAGGCAGCUAGAUGAGACCUCUUCCGAACCGACAGAUCU CGGGCAAGCCGGGCCUGGGCGCCUUUCCUCAGCCAGCAGUGAAGUCCAGGAG GAUAU	−	3	3	37.5	0
Δ 5 Sequence (nts 2150-2400): CUCGGCACCAUAGGGGUCCGGACUCCAUUUUAGGAUUCGCCCAUUCCUGUCU CUUCCUACCCAACCACUCAAUUAAUCUUUCCUUGCCUGAGACCAGUUGGAAG CACUGGAGUGCAGGGAGGAGAGGGAAGGGCCAGGCUGGGCCUGGCCAGGUUCUA GUCUCCUGUGCAUGAGGGCCACACAAACACCAUGAGAAGGACCUCGGAGGCU GAGAACUUAACUGCUGAAGACACGGACACUCCUGCCCUGCUG	−	7	4	44	0
GLUT4 (from Hind III site@nt 2338 to end of insert@nt 2500) :					
AGCUUCUGACCAACUAAGGGCGGGAGGGGAUUUGAAAGGCUGCCUAUAAACA CUGGUUGGGAGGGAGCCUUUGGUAUUUUUGUAUGAAGAACGGAUAGGGAGCA GAAACCCAAGGGCUGUAUUAAAUGUGUAUAUAGAGAUUCGUCCAUAAAGU	~	8	5	55.5	0

[a] All sequences are listed 5′ to 3′.
[b] Transcripts of the 5′-most 102 nt (51% A+U) and the 3′-most 40 nt (73% A+U) are individually bound by Hel-N1, with the greatest binding to the shorter, more A/U-rich 3′ end of the Δ1 sequence.

an approximate 2-fold (1.8 ± 0.15-fold) increase in the amount of GLUT1 mRNA was observed after days 4, 5, and 8 in the Hel-N1 transfectants in comparison to the untransfected cells (Fig. 6A). These results are consistent with the possibility that the increase in GLUT1 protein following transfection with Hel-N1 involves stabilization of the GLUT1 mRNA. Examination of the half-life of the GLUT1 message in untransfected and Hel-N1-expressing cells, using actinomycin D to inhibit transcription, is shown in Fig. 6B and C. In cells expressing Hel-N1, the GLUT1 message was markedly stabilized, exhibiting a half-life of 7.0 ± 0.5 h (mean ± SD, $n = 3$). The half-life of GLUT1 mRNA in the untransfected cells was determined to be 4.8 ± 0.3 h (mean ± SD, $n = 3$), which compares favorably to the 4.5 ± 1.7 h reported by Kaestner et al. (21). These data suggest that the accumulation of GLUT1 protein results from increased levels of GLUT1 mRNA, which corresponds with a significant stabilization of the message.

Functional assay of increased GLUT1 expression. The increased GLUT1 protein detected in the immunoblot analysis was confirmed by a functional assay of 2-deoxyglucose uptake. The Hel-N1 transfectants exhibited a threefold increase in the rate of glucose uptake compared to the wild-type cells (153 ± 10 pmol/min/10^6 cells for untransfected cells; 518 ± 73 pmol/min/10^6 cells for Hel-N1 transfectants). To determine whether this increased rate of glucose uptake could be attributed to the overexpression of GLUT1 in the stable transfectants, membrane fractionation was performed on day 8 untransfected and Hel-N1 transfected cells. Comparison of GLUT1 protein content in isolated total cellular membranes indicated an 8.3 ± 0.9-fold overexpression of the GLUT1 protein in the Hel-N1 transfectants. The sublocalization of the GLUT1 protein was

further investigated, as shown in a representative immunoblot prepared by using isolated plasma and microsomal membrane fractions (Fig. 7). Purification of the plasma membranes (approximately 28-fold purification with a 6.5% yield) and microsomal membranes (approximately 60-fold purification with a 10% yield) demonstrated a 3-fold increase in the GLUT1 protein content associated with the plasma membrane fraction relative to untransfected cells, consistent with the increased rate of 2-deoxyglucose uptake described above. The microsomal GLUT1 protein content in the transfectants increased 4.8 ± 0.8-fold, suggesting that a substantial portion of the GLUT1 antigen detected in the immunoblots represented protein in various stages of processing or sequestration.

GLUT1 mRNA distribution in polysome profiles following Hel-N1 transfection. Sucrose density gradient analysis was performed to determine if expression of Hel-N1 altered the distribution of GLUT1 mRNA among ribosomes and polysomes, thereby potentially affecting the rate of translation or half-life of the message. The analysis was performed on day 8 following induction of differentiation, and representative polysome profiles for untransfected 3T3-L1 cells (Fig. 8A) and Hel-N1 transfectants (Fig. 8B) are shown. A shift in the profile was observed in the Hel-N1-transfected cells in which GLUT1 mRNA was absent from fraction 4 (40S preinitiation complex) and fractions 5 to 6 (80S initiation complex). In comparison of several independent gradients, the GLUT1 mRNA distribution was consistently skewed toward the densest portion of the gradient, which contained polysomes with increasing numbers of ribosomes (fractions 10 to 16). While the bulk of the GLUT1 mRNA is localized to fractions 13 to 15 in both gradients (shaded portion in polysome profile), these fractions
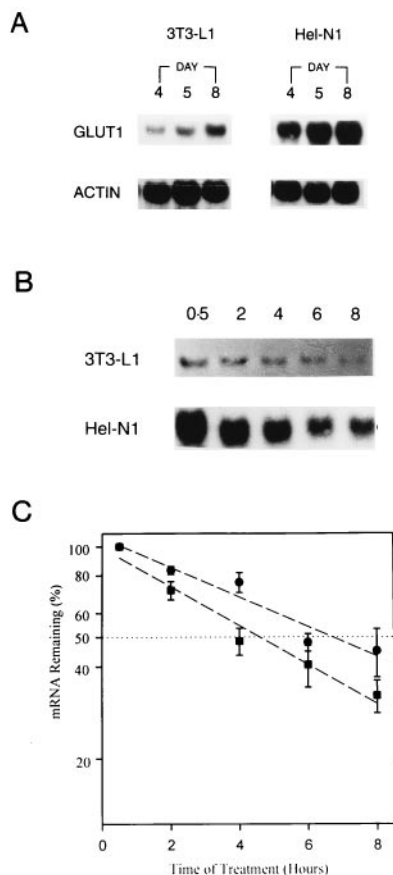
FIG. 6. Effect of Hel-N1 expression on GLUT1 mRNA accumulation and turnover. (A) Northern blot of RNA isolated from untransfected cells and stable transfectants on days 4, 5, and 8 of the differentiation time course. RNAs (20 μg/lane) were subjected to electrophoresis and analyzed as described in Materials and Methods. Blots were sequentially hybridized with cDNA probes corresponding to GLUT1 and β-actin. (B) On day 8 of a differentiation time course, the wild-type and Hel-N1-transfected cells were treated with actinomycin D (time zero), RNA was isolated at the indicated time points, and Northern blot analysis was performed for GLUT1 as described in Materials and Methods. (C) The hybridization patterns of six independent experiments were analyzed by densitometric scanning, quantified with Imagequant software (Molecular Dynamics), and plotted as mean percent mRNAs remaining in the untransfected 3T3-L1 cells (■) and Hel-N1 transfectants (●). The GLUT1 mRNA half-lives within experimental variation were calculated according to linear regression values to be 4.8 ± 0.7 h in 3T3-L1 and 7.0 ± 0.5 h in the Hel-N1 transfectants. The slopes of the two lines displayed were determined to be significantly different with $P < 0.0001$.
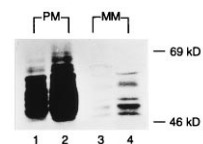

FIG. 7. Membrane distribution of GLUT1 protein in untransfected and Hel-N1 transfectants. Plasma membranes (PM) and microsomal membranes (MM) were isolated on day 8 of a differentiation time course from untransfected 3T3-L1 cells (lanes 1 and 3) and Hel-N1-transfected cells (lanes 2 and 4). The isolated membranes were subjected to immunoblot analysis as described in Materials and Methods. Densitometric quantification (Imagequant software; Molecular Dynamics) of the GLUT1 protein content associated with the plasma membrane and microsomal membrane fractions of Hel-N1 transfectants relative to untransfected cells demonstrated 3- and 4.8-fold increases, respectively.

characterization of the 3T3-L1 system over the last two decades, adipocyte differentiation has emerged as a model for studies of gene expression and terminal cell differentiation (9, 29). The combination of the 3T3-L1 cell line and successful expression of various forms of Hel-N1 permitted an approach to the functional analysis of this highly specialized RRM-containing protein.

GLUT1, a ubiquitously expressed glucose transporter, is a member of a multigene transporter family (33). In the 3T3-L1 fibroblasts, GLUT1 mRNA exhibits a half-life of 42 ± 9 min and behaves much like an immediate-early mRNA (8). However, as the cells differentiate and express the adipose phenotype, a marked stabilization of the half-life occurs increasing to 4.5 ± 1.7 h (21). This is particularly interesting in that quantifiable GLUT1 mRNA and protein content remain at or below the levels found in the undifferentiated cells, suggesting that a transcriptional down-regulation must compensate for the increased stability (42, 43). In the Hel-N1 transfectants, we have observed an increased accumulation of the GLUT1 mRNA, due in part to a further stabilization of the message (half-life of 7.0 ± 0.5 h), which then translates into an increased GLUT1 protein content. While both Hel-N1 and GLUT1 proteins are expressed in the uninduced transfected fibroblasts, the observed 8- to 10-fold increase in GLUT1 protein occurs only as the cells attain the adipocyte phenotype and only in the hormonally induced transfectants. This finding suggests that essential adipose-specific regulatory factors or proteins expressed as the cells differentiate are required to promote the Hel-N1-induced alteration of GLUT1 expression. With respect to the function of GLUT1, this regulation appears to signal an increased need for glucose during the differentiation process.

Use of RNA gel shift analysis and immunoprecipitation techniques demonstrated that in vitro, Hel-N1 bound specifically to a 130-nt AU-rich region of the GLUT1 3′UTR which we refer to as Δ1. It is interesting that the binding domain is within a 40-nt region (nt 1891 to 1930) which exhibits 100% homology between the human and murine GLUT1 mRNAs, suggesting functional importance through phylogenetic conservation.

While an 8- to 10-fold increase in GLUT1 protein was observed in the Hel-N1 transfectants, examination of the distribution of the protein indicated that only a 3-fold increase occurred at the plasma membrane. This corresponded well to the threefold increase in rates of basal glucose transport. It has been reported that transporters detected in association with the plasma membrane are largely active (47). However, Western blotting will also detect transport-inactive intermediates in normal transporter trafficking housed in plasma membrane-associated but occluded vesicles. These intermediates have

represented heavier polysomes which shifted into the smaller peak at the very bottom of the gradient in the Hel-N1 transfectants (Fig. 8B). The loss of detection of GLUT1 mRNA in the less dense fractions (fractions 4 to 6) of the gradient is consistent with an up-regulated loading of ribosomes onto GLUT1 mRNA in the cells expressing Hel-N1, indicating an acceleration in the initiation of translation.

DISCUSSION

Initial attempts to create stable transfectants which expressed Hel-N1 in various mammalian cell lines were precluded due to cell death or cytostasis. In this study, we successfully expressed Hel-N1 in 3T3-L1 preadipocytes. These cells, subcloned from mouse embryo fibroblasts, differentiate in monolayer culture into cells exhibiting the biochemical and morphological characteristics of adipocytes (9, 29). With the
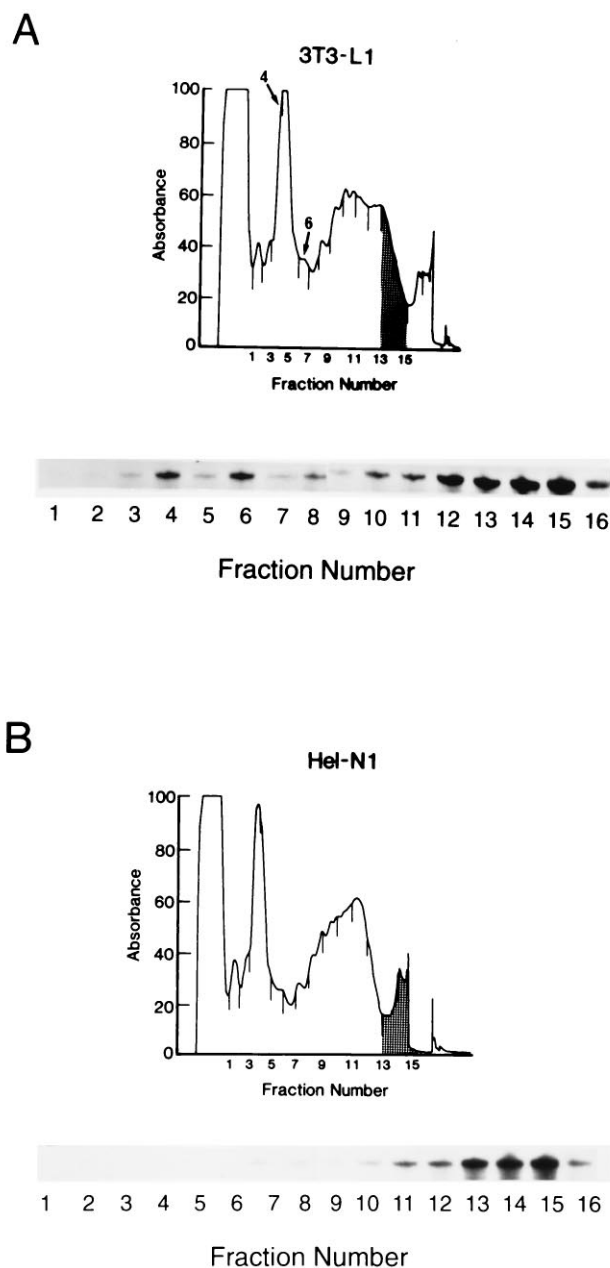
FIG. 8. Polysome profiles and GLUT1 localization. (A) A postmitochondrial supernatant was prepared from untransfected cells on day 8 of a differentiation time course and applied to a 15 to 45% sucrose density gradient, which was centrifuged at $20,000 \times g$ for 2 h. The gradients were fractionated, and the absorbance at 254 nm was measured, generating a polysome profile. The tops of the gradients are to the left. RNA from the fractions was isolated, and GLUT1 content was determined by RNase protection assay. (B) Identical analysis for Hel-N1 transfectants.

been suggested to contribute to a relatively small degree to total plasma membrane GLUT1 (47). The bulk of the increased GLUT1 appears to have been localized to the intracellular pool of transporters, similar to the finding of Yang et al. (47) that the decrease in the intrinsic activity of the GLUT1 transporter with respect to differentiation appeared to be due to transporter sequestration within the cell. These observations suggest that ectopic expression of Hel-N1, while altering the expression of GLUT1, did not alter the normal equilibrium

distribution of the transporter. Moreover, we suggest that it is the overexpression of GLUT1 at the plasma membrane which leads to the increased basal rate of transport, resulting in a 40% increase in stored triacylglycerol.

Detection of the broad GLUT1 band by Western analysis was inhibited by adsorption of the anti-GLUT1 antibody to an antigen affinity column. While confirming that the signal was generated by GLUT1 protein, this did not explain the apparent multiple forms observed. Differences in electrophoretic mobility on SDS-PAGE of immunoreactive GLUT1 have been demonstrated to arise from differences in the complexity of N-linked carbohydrate groups (26). Glycosylation of the GLUT1 transporter can be modulated by cytokines, growth factors such as transforming growth factor β1, and glucose deprivation, leading to the detection of multiple bands and/or broad bands (31, 34). The heterogeneity of glycosylation has been suggested to have a functional role in regulating glucose transporter kinetic activity or differential subcellular localization (26). In these situations, molecular size has been reported in the range from ~47 to 65 kDa (26, 31, 34). Thus, we suggest that alterations in the complexity of glycosylation of GLUT1 protein in the presence of Hel-N1 resulted in the broad, multiple-component band detected in our studies.

Polysome profile analysis demonstrated a Hel-N1-associated effect on translation. This technique permitted analysis of the association of the GLUT1 mRNA with the ribosomal subunits and polysomes, in both untransfected and Hel-N1-transfected 3T3-L1 adipocytes. The location of GLUT1 mRNA in the polysome profiles demonstrates a marked acceleration of the progression from the preinitiation complex to polysomes in the Hel-N1 transfectants, which suggests an enhancement of initiation. In addition, the bulk of the GLUT1 mRNA was associated with heavier (more dense) polysomes, consistent with an increased efficiency of ribosome loading and translation of this message. This interpretation is supported by studies on the translational regulation of *tra-2*, in which deletion of a negative control region from the 3′UTR led to an increased rate of translation coincident with movement of the message to the heavy (more dense) polysomes (17). This effect on the initiation of protein synthesis may result in both the stabilization of the GLUT1 mRNA and the increased synthesis of GLUT1 protein. These data suggest that control of translation, at the level of initiation, may be a major function of the Hel-N1 protein. However, the differentiation-specific requirement for Hel-N1-enhanced GLUT1 expression implies involvement of regulatory events other than just binding of Hel-N1 to the Δ1 region of the GLUT1 3′UTR.

While our studies have been conducted with adipocytes, it is important to note that Hel-N1 was originally cloned from a fetal human brain cDNA library and found to be highly homologous to the *D. melanogaster* neuronal protein ELAV, which functions in differentiation (27). In addition, examination of several human brain tumor cell lines by immunoblot analysis indicated the presence of high levels of endogenous human ELAV proteins (14). Interestingly, GLUT1 is expressed at high levels in neuronal tissues, the blood-brain barrier, and the brain (30). The coexistence of Hel-N1 and GLUT1 mRNAs in the brain suggests that these molecules may interact in vivo and that Hel-N1 may function in neuronal differentiation as it does in adipogenesis.

The differentiation-dependent overexpression of GLUT1, potentially resulting from a direct interaction of Hel-N1 with the 3′UTR of its mRNA, is consistent with the increased metabolic needs of the transfected cell as it begins to synthesize and store lipid at an enhanced rate. Although the precise mechanism of its effects on cell growth and protein expression

will require further study, our data provide support for a role for Hel-N1 in translational efficiency as well as message stability.

REFERENCES

1. **Antic, D., and J. D. Keene.** Messenger ribonucleoprotein complexes containing human ELAV proteins in proliferating and differentiating cells of neuronal origin. Submitted for publication.
2. **Ausubel, F. M., R. Brent, R. E. Kingston, D. D. Moore, J. G. Seidman, J. A. Smith, and K. Struhl (ed.).** 1995. Current protocols in molecular biology. John Wiley and Sons Inc., New York, N.Y.
3. **Casey, J. L., M. W. Hentze, D. M. Koeller, S. W. Caughman, T. A. Rouault, R. D. Klausner, and J. B. Harford.** 1988. Iron-responsive elements: regulatory RNA sequences that control mRNA levels and translation. Science **240:**924–928.
4. **Chirgwin, J. M., A. E. Przybyla, R. J. MacDonald, and W. J. Rutter.** 1979. Isolation of biologically active ribonucleic acid from sources enriched in ribonuclease. Biochemistry **18:**5294–5299.
5. **Chung, S., L. Jiang, S. Cheng, and H. Furneaux.** 1996. Purification and properties of HuD, a neuronal RNA-binding protein. J. Biol. Chem. **271:** 11518–11524.
6. **Cleveland, D. W., M. A. Lopata, R. J. MacDonald, N. J. Cowan, W. J. Rutter, and W. J. Kirschner.** 1980. Number and evolutionary conservation of alpha and beta tubulin and cytoplasmic beta- and gamma-actin genes using specific cloned cDNA probes. Cell **20:**95–105.
7. **Cornelius, P., M. Marlowe, M. D. Lee, and P. H. Pekala.** 1990. The growth factor like effects of tumor necrosis factor-α: stimulation of glucose transport activity and induction of glucose transporter and immediate early gene expression. J. Biol. Chem. **265:**20506–20516.
8. **Cornelius, P., M. Marlowe, K. Call, and P. H. Pekala.** 1991. Regulation of glucose transport as well as glucose transporter and immediate early gene expression in 3T3-L1 preadipocytes by 8-bromo-cAMP. J. Cell. Physiol. **146:**298–308.
9. **Cornelius, P., O. M. MacDougald, and M. D. Lane.** 1994. Regulation of adipocyte development. Annu. Rev. Nutr. **14:**99–129.
10. **Cullen, B.** 1986. Transactivation of human immunodeficiency virus occurs via a bimodal mechanism. Cell **46:**973–982.
11. **Frost, S. C., and M. D. Lane.** 1985. Evidence for the involvement of vicinal sulfhydryl groups in insulin-activated hexose transport by 3T3-L1 adipocytes. J. Biol. Chem. **260:**2646–2652.
12. **Fushiki, T., J. A. Wells, E. B. Tapscott, and G. L. Dohm.** 1989. Changes in glucose transporters in muscle in response to exercise. Am. J. Physiol. **256:** E580–E587.
13. **Gallie, D. R., and V. Walbot.** 1990. RNA pseudoknot domain of tobacco mosiac virus functionally substitute for a poly(A) tail in plant and animal cells. Genes Dev. **4:**1149–1157.
14. **Gao, F., C. C. Carson, T. Levine, and J. D. Keene.** 1994. Selection of a subset of mRNAs from a combinatorial 3′ untranslated region libraries using neuronal RNA-binding protein Hel-N1. Proc. Natl. Acad. Sci. USA **91:**11207–11211.
15. **Gao, F.-B., and J. D. Keene.** 1996. Hel-N1/Hel-N2 proteins are bound to poly(A)⁺ mRNA in granular RNP structures and are implicated in neuronal differentiation. J. Cell Sci. **109:**579–589.
16. **Good, P. J.** 1995. A conserved family of *elav*-like genes in vertebrates. Proc. Natl. Acad. Sci. USA **92:**4557–4561.
17. **Goodwin, E. B., T. G. Okkema, T. C. Evans, and J. Kimble.** 1993. Translational regulation of *tra-2* by its 3′ untranslated region controls sexual identity in *C. elegans*. Cell **75:**329–339.
18. **Hu, X., and K. S. Zukerman.** 1995. Isolation of full-length cDNA encoding the common β-subunit of GM-CSF, IL-3 and IL-5 receptors by RT-PCR. Focus **17:**21–24.
19. **Jain, R. G., and P. P. Pekala.** 1996. Unpublished data.
20. **Kaestner, K. H., R. J. Christy, J. C. McLenithan, L. T. Braiterman, P. Cornelius, P. H. Pekala, and M. D. Lane.** 1989. Sequence, tissue distribution and differential expression of mRNA for a putative insulin-responsive glucose transporter in mouse 3T3-L1 adipocytes. Proc. Natl. Acad. Sci. USA **86:**3150–3154.
21. **Kaestner, K. H., J. R. Flores-Riveros, J. C. McLenithan, M. Janicot, and M. D. Lane.** 1991. Transcriptional repression of the mouse insulin-responsive glucose transporter (GLUT4) gene by cAMP. Proc. Natl. Acad. Sci. USA **88:**1933–1937.
22. **Kern, M., J. A. Wells, J. M. Stephens, C. W. Elton, J. E. Freidman, E. D. Tapscott, P. H. Pekala, and G. L. Dohm.** 1990. Insulin responsiveness in skeletal muscle is determined by glucose transporter (GLUT4) protein level. Biochem. J. **270:**397–400.
23. **King, P. H., T. D. Levine, R. T. Fremeau, Jr., and J. D. Keene.** 1994. Mammalian homologue of *Drosophila* ELAV localized to a neuronal subset can bind in vitro to the 3′UTR of mRNA encoding the Id transcriptional repressor. J. Neurosci. **14:**1943–1952.
24. **Klip, A., and D. Walker.** 1983. Insulin binding to differentiating muscle in culture. Arch. Biochem. Biophys. **221:**175–187.
25. **Kruys, V., M. G. Wathelet, and G. A. Huez.** 1988. Identification of a translation inhibitory element (TIE) in the 3′ untranslated region of the human interferon-β mRNA. Gene **72:**191–200.
26. **Kumagai, A. K., J. D. Dwyer, and W. M. Pardridge.** 1994. Differential glycosylation of the GLUT1 glucose transporter in brain capillaries and choroid plexus. Biochim. Biophys. Acta **1193:**24–30.
27. **Levine, T. D., F. Gao, P. H. King, L. G. Andrews, and J. D. Keene.** 1993. Hel-N1: an autoimmune RNA-binding protein with specificity for 3′ uridylate-rich untranslated regions of growth factor mRNAs. Mol. Cell. Biol. **13:**3494–3504.
28. **Long, S. D., and P. H. Pekala.** 1996. Regulation of GLUT4 mRNA stability by TNFα: alterations in both protein binding to the 3′ untranslated region and initiation of translation. Biochem. Biophys Res. Commun. **220:**949–953.
29. **MacDougald, O. A., and M. D. Lane.** 1995. Transcriptional regulation of gene expression during adipocyte differentiation. Annu. Rev. Biochem. **64:** 345–373.
30. **Maher, F., S. J. Vannucci, and I. A. Simpson.** 1994. Glucose transporter proteins in the brain. FASEB J. **8:**1003–1011.
31. **Masumi, A., Y. Akamatsu, and T. Kitagawa.** 1993. Modulation of the synthesis and glycosylation of the glucose transporter protein by transforming growth factor-β1 in Swiss 3T3 fibroblasts. Biochim. Biophys. Acta **1145:**227–234.
32. **McCarthy, J. E., and H. Kollmus.** 1995. Cytoplasmic mRNA-protein interactions in eukaryotic gene expression. Trends Biochem. Sci. **20:**191–197.
33. **McGowan, K. M., S. D. Long, and P. H. Pekala.** 1995. Glucose transporter gene expression: regulation of transcription and mRNA stability. Pharmacol. Ther. **66:**465–505.
34. **McMahon, R. J., and S. C. Frost.** 1995. Nutrient control of GLUT1 processing and turnover in 3T3-L1 adipocytes. J. Biol. Chem. **270:**12094–12099.
35. **Murata, Y., and R. P. Wharton.** 1995. Binding of *pumilio* to maternal *hunchback* mRNA is required for posterior patterning in *Drosophila* embryos. Cell **80:**747–756.
36. **Ostareck-Lederer, A., D. H. Ostareck, N. Standart, and B. J. Thiele.** 1994. Translation of 15-lipoxygenase mRNA is inhibited by a protein that binds to a repeated sequence in the 3′ untranslated region. EMBO J. **13:**1476–1481.
37. **Pandey, N. B., and W. F. Marzluff.** 1987. The stem-loop structure at the 3′ end of the histone mRNA is necessary and sufficient for regulation of histone mRNA stability. Mol. Cell. Biol. **7:**4557–4559.
38. **Pekala, P., M. Kawakami, W. Vine, M. D. Lane, and A. Cerami.** 1983. Studies of insulin resistance in adipocytes induced by a macrophage mediator. J. Exp. Med. **157:**1360–1365.
39. **Query, C. C., R. C. Bentley, and J. D. Keene.** 1989. A common RNA recognition motif identified within a defined U1RNA binding domain of the 70K U1 snRNP protein. Cell **57:**89–101.
40. **Romac, J. M., D. H. Graff, and J. D. Keene.** 1994. The U1 small nuclear ribonucleoprotein (snRNP) 70K protein is transported independently of U1 snRNP particles via a nuclear localization signal in the RNA-binding domain. Mol. Cell. Biol. **14:**4662–4670.
41. **Shaw, G., and R. Kamen.** 1986. A conserved AU sequence from the 3′ untranslated region of GM-CSF mRNA mediates selective mRNA degradation. Cell **46:**659–667.
42. **Stephens, J. M., and P. H. Pekala.** 1991. Transcriptional repression of the C/EBPα and GLUT4 genes in the 3T3-L1 adipocytes by tumor necrosis factor-α. J. Biol. Chem. **266:**21839–21845.
43. **Stephens, J. M., and P. H. Pekala.** 1992. Transcriptional repression of the C/EBPα and GLUT4 genes in the 3T3-L1 adipocytes by tumor necrosis factor-α. Regulation is coordinate and independent of protein synthesis. J. Biol. Chem. **267:**13580–13584.
44. **Studier, F. W., and B. A. Moffatt.** 1986. Use of bacteriophage T7 RNA polymerase to direct selective high-level expression of cloned genes. J. Mol. Biol. **189:**113–130.
45. **Tebbey, P. W., K. M. McGowan, J. M. Stephens, T. M. Buttke, and P. H. Pekala.** 1994. Arachidonic acid down-regulates the insulin-dependent glucose transporter (GLUT4) in 3T3-L1 adipocytes by inhibiting transcription and enhancing mRNA turnover. J. Biol. Chem. **269:**639–644.
46. **Tsai, D. E., D. J. Kenan, and J. D. Keene.** 1992. In vitro selection of an RNA epitope immunologically cross-reactive with a peptide. Proc. Natl. Acad. Sci. USA **89:**8864–8868.
47. **Yang, J., A. E. Clark, I. J. Kozka, S. W. Cushman, and G. D. Holman.** 1992. Development of an intracellular pool of glucose transporters in 3T3-L1 cells. J. Biol. Chem. **267:**10393–10399.